N. Rijova, V. Saraeva, K. Gantchev, I. Bakalov, H. Wolff and *S. Arndt*

Analysis of the melt spreading and MCCI during the ex-vessel phase of a severe accident in WWER-1000

The paper presents analysis results of melt spreading and core-concrete interactions in the containment of a WWER-1000 plant during the ex-vessel phase of a severe accident. The failure of the vessel takes place 8 h 35 min after the initiation of the accident. It has been assumed that the whole area of the containment floor is available for spreading, i. e. the door between the reactor cavity and the main part of the containment is not locked. The melt flow rate from the reactor pressure vessel was used as a boundary condition. The simulation of the melt spreading was performed with the LAVA code. The calculated spreading area varies from 60 to 100 m^2 depending on the assumed values of the melt properties. The results from the LAVA calculations were used in parallel for COCOSYS and MELCOR calculations to study the core-concrete interactions. From the analyses it turned out: a larger spreading area leads to a faster cooling of the melt in the initial period of the accident, but in the long term the temperatures are the same. 60 h after start of the ex-vessel phase, the melt is not stabilised.

Analyse der Schmelzeausbreitung und der Schmelze-Beton-Wechselwirkung (MCCI) während der Ex-Vessel-Phase eines Kernschmelzunfalls in einem WWER-1000. *Dieser Beitrag stellt Ergebnisse von Rechnungen zur Schmelzeausbreitung und zur Schmelze-Beton-Wechselwirkung im Containment einer WWER-1000-Anlage während der Ex-Vesselphase eines schweren Unfalls vor. Dabei versagt der Reaktordruckbehälter 8 Stunden 35 Minuten nach dem Beginn des Unfalls. Es wurde angenommen, dass der gesamte Bereich des Containment-Bodens für die Ausbreitung der Schmelze zur Verfügung steht, d. h. die Tür zwischen der Reaktorgrube und dem Hauptteil des Containments ist nicht verriegelt. Als Randbedingung wurde der Massenstrom der Schmelze aus dem Reaktordruckbehälter heraus verwendet. Die Berechnung der Schmelzeausbreitung erfolgte mit dem Programm LAVA. Die berechnete Ausbreitungsfläche variiert zwischen 60 und 100 m^2 in Abhängigkeit von den angenommenen Schmelzeeigenschaften. Die Ergebnisse der LAVA-Berechnungen gingen als Anfangs- und Randbedingungen in die anschließenden Berechnungen mit den Programmen COCOSYS und MELCOR ein. Mit diesen wurden die Schmelze-Beton-Wechselwirkungen berechnet. Diese Rechnungen zeigten, dass ein größerer Ausbreitungsbereich zu einer schnelleren Abkühlung der Schmelze in der Anfangsphase des Unfalls führt. Langfristig verschwindet der Einfluss der Ausbreitungsfläche, d. h. die berechneten Temperaturen sind gleich. Es zeigt sich, dass 60 Stunden nach Beginn der Ex-Vesselphase die Schmelze noch nicht stabilisiert ist.*

1 Introduction

The Fukushima Daiichi disaster and the results of the following stress tests of European NPPs have revealed the increased necessity of elaboration and verification of additional measures related to severe accident management. The verification of severe accident management procedures requires the availability of validated codes and corresponding input decks for modelling the phenomena that take place during severe accidents. In the last five years input decks have been developed for the modelling of melt spreading and MCCI during a severe accident at a WWER-1000 plant. The LAVA and CCI codes have been used for the melt spreading and MCCI respectively. Both codes are modules of COCOSYS [1] (which itself is a part of the AC^2 code complex). LAVA can be applied as a standalone code.

The spreading of melt increases the cooling surface and thus the cooling rate of the melt. If the melt layer is thin enough to be coolable, i. e. the decay heat can be removed to the surrounding air and to the structures, the MCCI will stop and there will be no threat to the containment integrity.

The WWER-1000 reactor cavity is connected to the main part of the containment via a heavy steel door, designed to withstand pressure difference of 0.49 MPa. It is locked during normal operation of the reactor facility. The reactor cavity has relatively small volume – 177 m^3 and is not directly connected to the containment. Owing to these features, the direct containment heating is considered to be of low probability (see Chapter IV of [5]).

Calculations performed earlier show that a failure of the steel door or surrounding structures takes place approximately 10 h after the failure of the reactor pressure vessel. By this time, the basement plate of the reactor cavity is significantly destroyed due to the MCCI and a collapse under the weight of the melt cannot be excluded.

The possibility of keeping the door between the reactor cavity and the containment closed but unlocked during normal reactor operation is under discussion. It is assumed that this measure will let the corium spread to a broader area and, possibly, become coolable. Even if this is proved, additional investigation is necessary to evaluate the consequences of possible DCH, since the opening of the door changes the conditions under which the mentioned above studies [4–6] are performed.

The first aim of the current study is to investigate the melt spreading in the WWER-1000 containment during the ex-vessel phase of a severe accident considering the whole area of the containment floor as spreading area. The LAVA code [2] was used for simulation of the core melt spreading and relocation in the containment.

In parallel, a MELCOR model of WWER-1000 (reference plant Kozloduy Units 5 and 6) is being developed and applied for an integral modelling of severe accidents, comprising the processes in the reactor pressure vessel and in the containment. This gives an opportunity for the parallel application of AC^2 modules and MELCOR. The second aim of the study is to perform a code-to-code verification of COCOSYS/CCI and MELCOR.

The evaluation of the DCH is out of the scope of the study and the corresponding models were applied neither in MELCOR, nor in COCOSYS calculations.

The MELCOR code does not comprise a physical model for the melt spreading. The spreading area has to be defined by the user. Thus, some external (outside MELCOR) evaluation of the spreading process is needed. In the current investigation, the LAVA results for the spreading area were used as a boundary condition for both MELCOR and COCOSYS calculations of the MCCI process.

The parameters of the melt, outflowing from the failed reactor pressure vessel and spilling on the floor of the reactor cavity and further in the other compartments of the containment, are taken from an earlier MELCOR investigation. A LAVA calculation is performed to evaluate the spreading area. The results are further used in parallel COCOSYS and MELCOR calculations to investigate the MCCI during the melt spreading and after the immobilization of the melt. A scheme of the stages of the investigation and corresponding successive calculations is presented in Fig. 1.

2 Scenario of the accident and results of the MELCOR calculation of the in-vessel phase of the accident

The station blackout (SBO) event at full power operation has been chosen as a representative severe accident scenario for the present study. The loss of all normal and emergency sources of AC power supply is a beyond design basis accident for WWER-1000. It leads to the generation of a reactor scram signal at the very first second of the accident. It also causes closing of the turbine stop valves, trip of the MCPs, switching off of the pressurizer's heaters, and loss of the primary make-up system. During the first 45 min the decay heat is transferred to the steam generators and released into the atmosphere. Since no feed water is supplied to the steam generators, their level decreases. The decay heat transfer to the secondary side becomes insufficient and the pressure in the primary circuit starts to increase. The first opening of the first pressurizer safety valve takes place approximately 50 min after the loss of power supply. Since that moment, the parameters in the containment start to change noticeably. Further, the first pressurizer safety valve periodically opens to maintain the primary pressure below 18.7 MPa. When the reactor water mass reaches approximately one third of the initial value, the cladding temperature starts to rise. The exothermic steam-Zirconium reaction accelerates and becomes self-sustaining. This is the beginning of the failure of fuel rods and of the in-vessel phase of the severe accident. A fast temperature excursion takes place 2 h and 40 min after the beginning of the accident. Around the third hour the coolant temperature in the upper plenum reaches 650 °C. According to severe accident management guidelines (SAMG), the operator opens the first safety valve of the pressuriser in order to avoid the failure of the reactor pressure vessel at high pressure. The decrease of the primary pressure after the opening of the safety valve allows the hydroaccumulators to inject water into the core. The injection does not prevent the severe accident, because by that time the core damage and relocation have already started. The vessel failure takes place 8 h and 35 min after start of the accident.

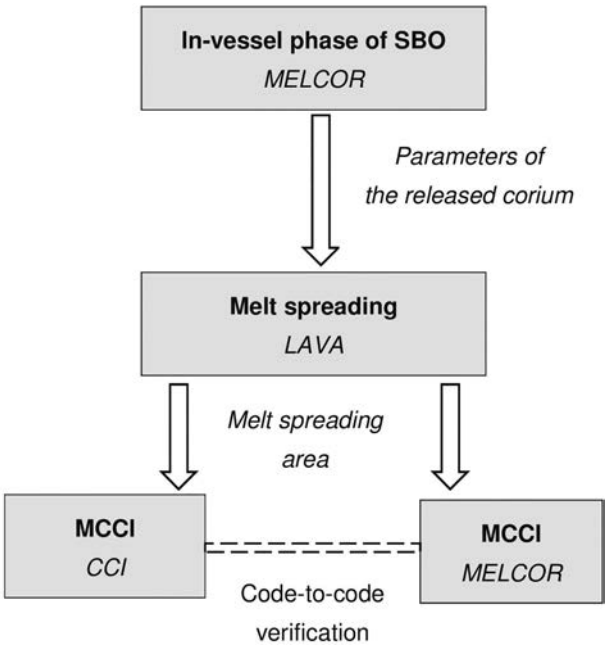

Fig. 1. Stages of the investigation

3 LAVA analysis of the melt spreading

The code LAVA is written for the simulation of melt spreading on extended surface structures driven by the force of gravity [2]. The validation of LAVA is based on COMAS-EU4, KATS-7 (see [2]) and ECOKATS-1 (see [6] page 367, [7]) experiments.

3.1 Geometry of the spreading area

The reactor cavity GA301 is designed in a cylindrical shape and is connected to the neighbouring compartment GA302 through a corridor and a hermetic steel door. The floor area of the cylindrical part and the corridor is 35.89 m^2. A layout of the reactor cavity GA301 and its neighbouring compartment GA302 is presented in Fig. 2. The cavity door is closed and the door setscrews are tightened up during normal operation. For the current study the door is assumed to be closed but unlocked. At the moment of the reactor pressure vessel failure the pressure in the cavity increases and the unlocked door opens. This assumption allows the melt to spread on a broader area and, possibly, to ensure a good melt coolability. The compartment GA302 is open to the annular corridor (GA308). The annular corridor includes the floor area around the fuel transportation hatch (GA303) and is connected to some other compartments. The total floor area available for spreading at the elevation of the reactor cavity is approximately 1 000 m^2. For the purposes of the current study, a reduced spreading area of about 428 m^2 was assumed. The layout of the reactor cavity and its neighbouring compartment as well as the annular corridor with the other associated rooms is presented in Fig. 3. The solid dark grey area depicts the modelled virtual boundaries of the spreading area for melt relocation in the containment compartments. The figure also depicts the boundaries of the fuel trans-

portation hatch (GA303) in the containment, which has a concrete 50 cm high pedestal.

A view of the LAVA computational grid representing the spreading area boundaries (solid bold line) is given in Fig. 4.

3.2 Initial and boundary conditions

Most of the input parameters of the melt in LAVA are calculated by MELCOR. Some of them can be found in different open sources as well. One of the most important rheological properties of the melt is viscosity. There are different options for the definition of the viscosity in LAVA. The first one is to specify a constant value. The other one is to specify a constant value for the viscosity of the liquid phase and to choose between the Arrhenius and Stedman model for calculation of the mushy viscosity. The mushy viscosity accounts for the solid fraction of the melt. The final value of the viscosity, so called apparent viscosity, accounts also for the void fraction, or the fraction of gases, generated during the MCCI and increasing the viscosity of the melt.

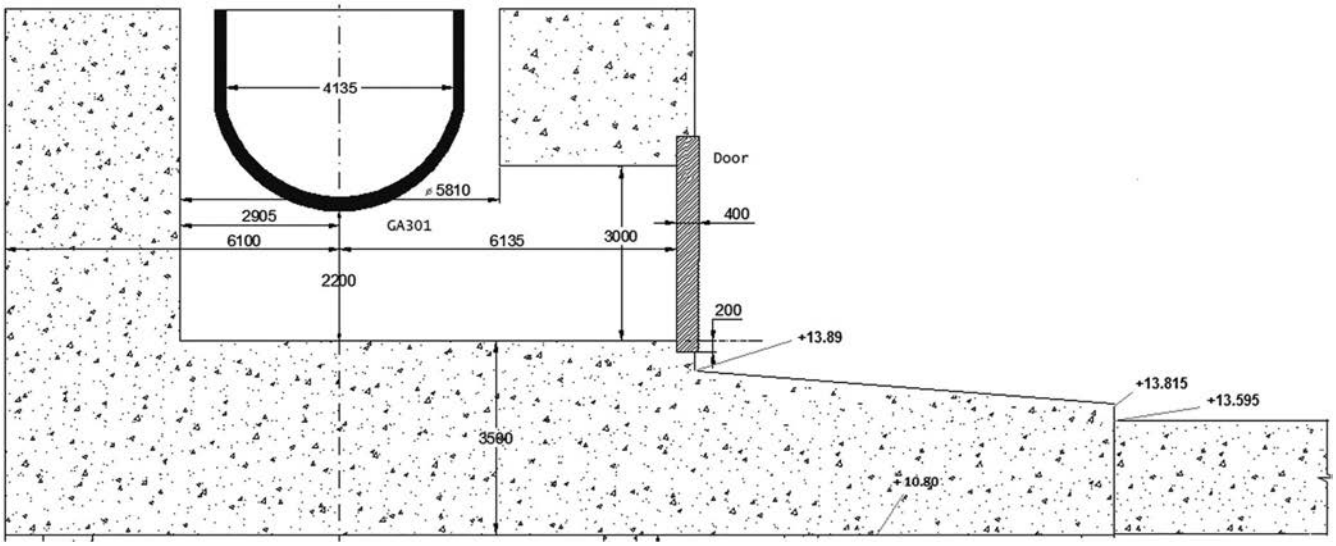

Fig. 2. Layout of reactor cavity GA301 and its neighbouring compartment GA302

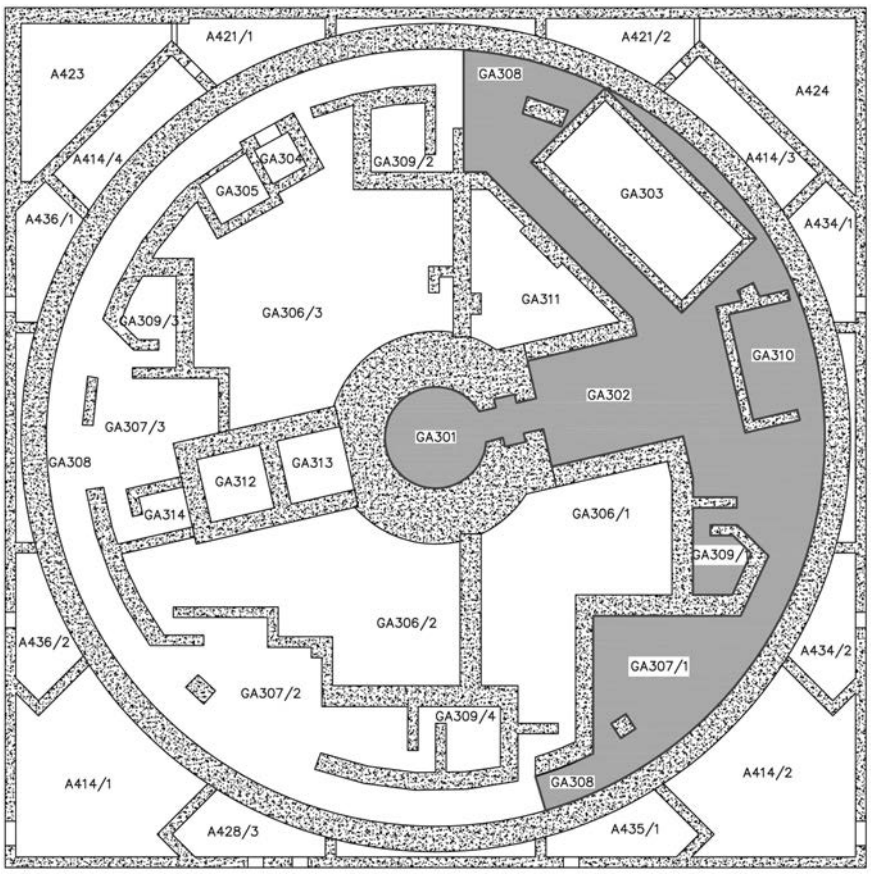

Fig. 3. Layout of the reactor cavity and its neighbouring containment rooms with marked spreading area

The current LAVA study includes two main cases with different input and boundary conditions. The second one is subdivided into three sub-cases. They are listed below:

- Calculation MEL_const: the main input parameters (the density and the specific heat capacity of the melt) are taken from the MELCOR calculation. The mushy viscosity is constant (the value is also taken from MELCOR);
- Calculations CALC_xxxx: the input parameters are determined, using different experimental data from open sources. The mushy viscosity is either defined or calculated, using different LAVA options:
  - Calculation CALC_const: the mushy viscosity is constant (the value is taken from MELCOR)
  - Calculation CALC_Arrh: Arrhenius correlation is used for the mushy viscosity

$$\eta(T) = \eta_0 \exp\left(2.5 C_\eta \varphi_s(T)\right)$$

where η_0 is the initial viscosity, C_η an empirical constant and φ_s the solid fraction.

  - Calculation CALC_Sted: Stedman correlation is used for the mushy viscosity

$$\eta(T) = \eta_0 \left(1 + \frac{0.75 \frac{\varphi_s}{\varphi_{s,max}}}{1 - \frac{\varphi_s}{\varphi_{s,max}}}\right)$$

where η_0 is the initial viscosity, φ_s the solid fraction and $\varphi_{s,max}$ the maximum solid fraction

According to the MELCOR code results, the core melt is injected into the reactor cavity within 10400 s (2.89 h). During the first hour, more than 80 % of the core melt is injected into the reactor cavity. Having in mind the rather long time of the LAVA calculations for the modelled geometry (more than 10 days for some cases) it was decided to shorten the melt release time. A constant flowrate equal to 17.26 kg/s was assumed. Figure 5 shows the melt injection assumed for the LAVA calculation in comparison with the MELCOR result.

In the LAVA calculations, an Ishihara's simple approach for the heat losses by radiation from the melt free surface is used. This approach assumes that the surface temperature is about 300 K lower than the maximum temperature of the melt mixture. This is based on experimental observations for volcanic lava flows [2].

3.3 LAVA melt spreading results

The results of the LAVA calculations are presented in Fig. 6. The comparisons of the covered area from the four variants is presented in Fig. 7. It can be seen that:

- For three of the calculations (MEL_const, CALC_const and CALC_Sted), the melt covers approximately the same area – about 90 ÷ 100 m^3 and the average melt thickness is about 0.25 ÷ 0.27 m;
- For calculation CALC_Arrh the melt covered area is about 60 m^3 and the average melt thickness is about 0.4 m;
- The biggest covered area is achieved in calculation MEL_const (97.7 m^2) and the smallest – in calculation CALC_Arrh (60.0 m^2);
- The melt spreads faster in calculation MEL_const and CALC_const;
- The spreading of the melt stops fastest in calculations CALC_const and CALC_Arrh (about 330 s), and last in calculation CALC_Sted (about 590 s).

As mentioned above, three of the calculated variants give approximately the same covered area, although they have a different shape. The front of the covered area is near to the transportation corridor lid and its reaching cannot be excluded. The melt is immobilized after about 5 to 10 min. The variants where the viscosity is constant have a similarity in the change of the covered area. Variants that take into account the change in viscosity over time as a result of temperature changes have a stepwise character of the increase in the

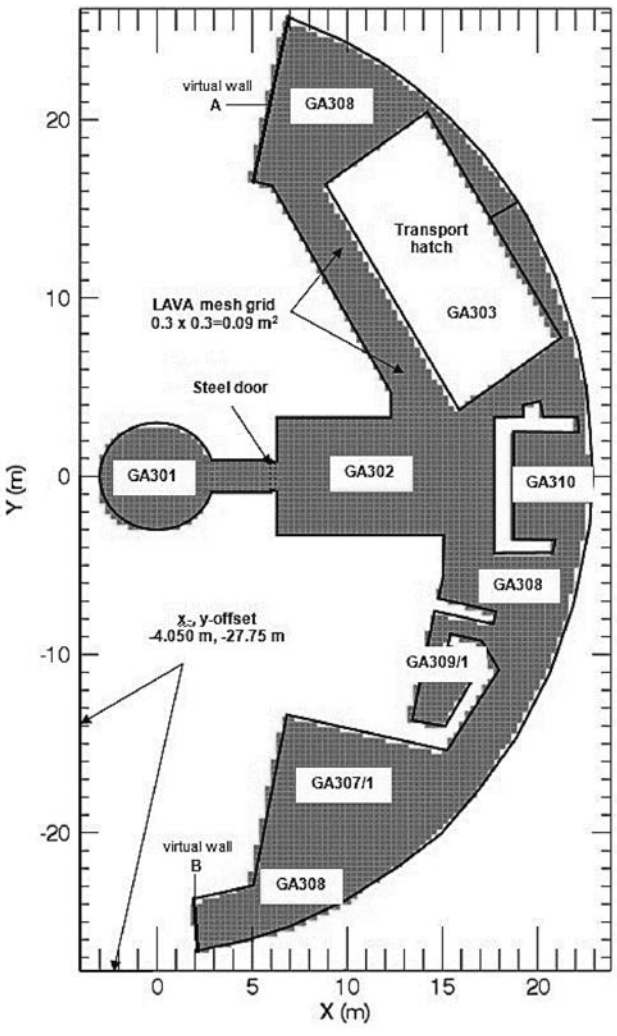

Fig. 4. LAVA computational grid for the melt spreading area

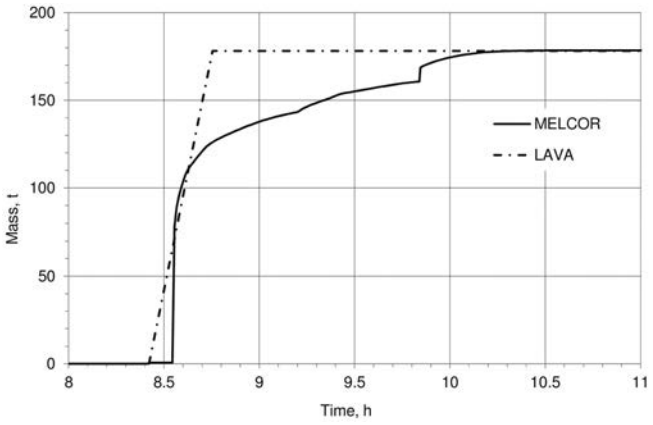

Fig. 5. Melt mass injection assumed for the LAVA calculations

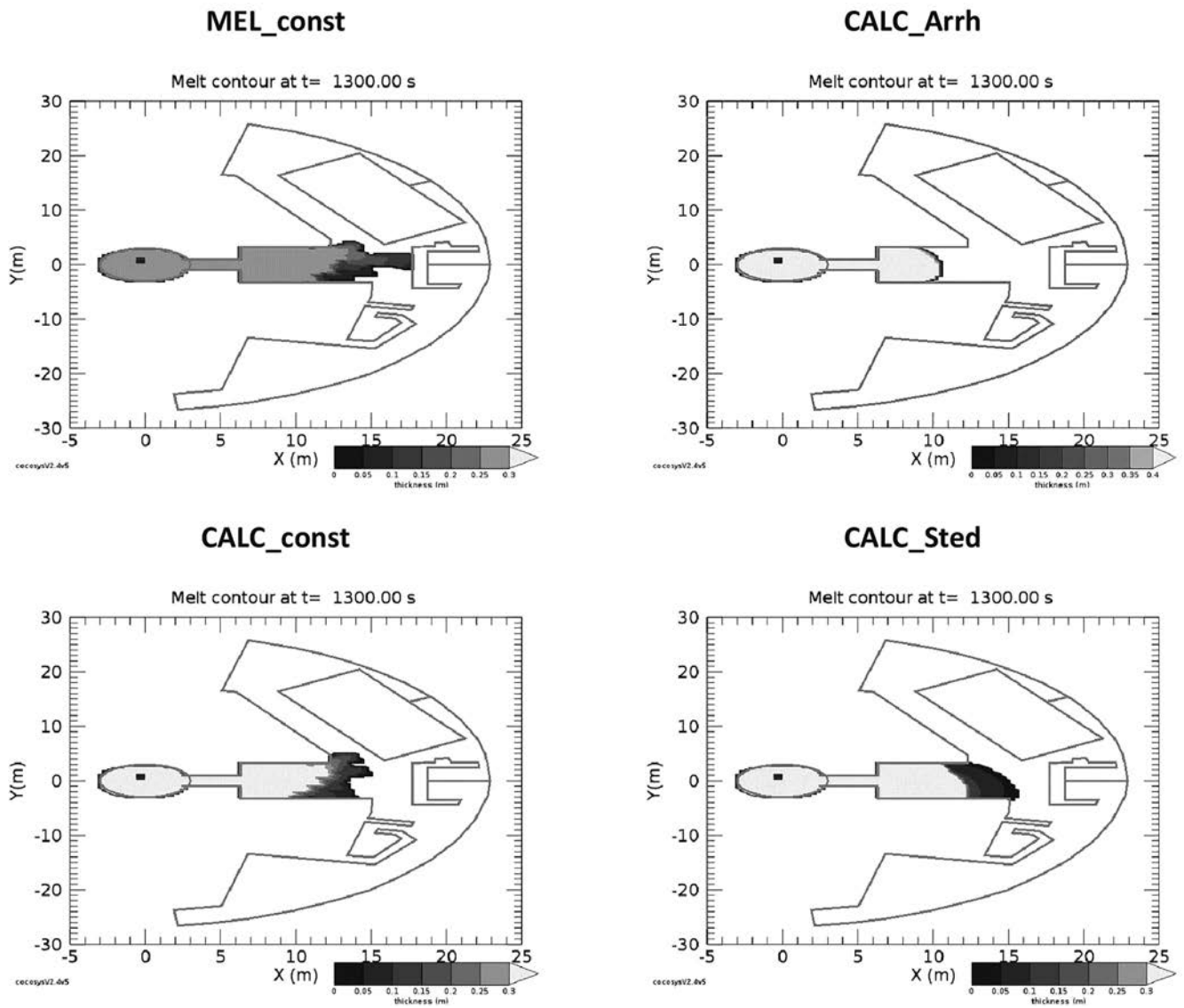

Fig. 6. LAVA melt spreading results

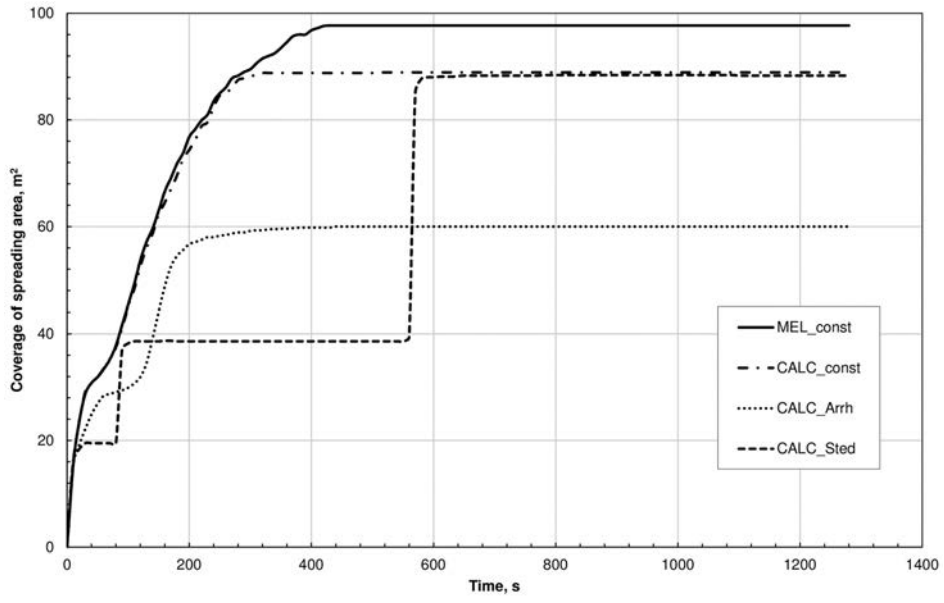

Fig. 7. Comparison of the covered area for calculated variants

covered area (more distinct in case CALC_Sted, less in CALC_Arrh).

4 Analysis of the MCCI

The analysis of the MCCI in the reactor cavity is performed applying both COCOSYS and MELCOR codes. Two groups of calculations were performed – one for a spreading area equal to 60 m^2 and a second one for 100 m^2. In each group of calculations, different assumptions for the initial configuration of the melt are made.

4.1 Short description of the COCOSYS and MELCOR MCCI modules

The COCOSYS MCCI module CCI [1] uses a lumped parameter approach and is based on a layer averaged description of the pool configuration. For each existing layer, mass balance equations are written per chemical element and the energy balance equation considers specific enthalpies per mass unit at each elemental mass composition of the layer, which allows to solve mass and energy balance equations independently of the detailed corium chemistry evolution. The CCI module comprises homogeneous, stratified and evolutionary configurations of the melt. In the homogeneous model the metals and the heavy oxides from the molten core materials are homogeneously mixed with the metals and light oxides from the ablated concrete. In the stratification model it is assumed that the metals from the molten core and the metals from the ablated concrete are mixed and stratified on the bottom of the melt pool. The heavy oxides from the molten core and the light oxides from the ablated concrete are fully mixed and stratified in the top part of the melt pool. Evolutionary means that the configuration of the melt can change from homogeneous to stratified. The process depends on the differ-

Table 1. Models and assumptions in MELCOR/CORCON and COCOSYS/CCI calculations

Model/Parameter		MELCOR/CORCON	COCOSYS/CCI
Cavity Geometry		Flat-bottom cylinder	Flat-bottom cylinder
Heat generation		Decay heat and chemical reactions	Decay heat (from MELCOR calculation) as boundary condition
Heat transfer between the pool top surface and the atmosphere		Convection with constant code defined HTC = 10 W/(m^2K) Thermal radiation with constant code defined emissivity factor 0.6	Convection with HTC at top melt surface calculated by the code (15 ÷ 20 W/(m^2K)) Thermal radiation with constant user defined emissivity factor (recommended values 0.35 for metal layer, 0.9 for oxide layer)
Heat transfer at melt pool/concrete interfaces		HTC **calculated** by the code: HTC = 1 244 ÷ 3 000 W/(m^2K) for the mixed layer of the homogeneous melt configuration during the initial phase of the MCCI. HTC = 1 000 ÷ 5 286 W/(m^2K) for the layers of the stratified melt configuration during the initial phase of the MCCI. HTC = 1 000 W/(m^2K) for the mixed layer of the homogeneous melt configuration during the late quasi-stationary phase of the MCCI. HTC = 1 000 W/(m^2K) for the oxide layer of the stratified melt configuration during the late quasi-stationary phase of the MCCI. HTC = 2 253 W/(m^2K) for the metal layer of the stratified melt configuration during the late quasi-stationary phase of the MCCI for the case with 60 m^2. HTC = 4 091 W/(m^2K) for the metal layer of the stratified melt configuration during the late quasi-stationary phase of the MCCI for the case with 100 m^2.	Constant user defined HTC: HTC = 500 W/(m^2K) for oxide layer in all directions HTC = 500 W/(m^2K) for metal layer in downward axial direction HTC = 1 000 W/(m^2K) for metal layer in upward axial and in radial direction
Melt configuration	Top surface	Liquid melt or crust	Similar crust model as in CORCON. Quasi-steady conduction through a crust is considered if $T_{interface} < T_{sol}$ Use of approximation of convective heat at the melt/crust interface driven by $h_{eff,up}$
	Melt	Homogeneous: metals and oxides are mixed into a single layer Stratified: up to three layers may exist – metal, heavy oxides below the metal, and light oxides above the metal	Homogeneous: metals and oxides are mixed into a single layer Stratified: two layers: metal on the bottom, oxide on the top Evolutionary: the criteria for stratification is calculated by the code, taking into account a user defined coefficient.
	Bottom and side surface	Liquid melt or crust	No crust is modelled
Concrete decomposition temperature		1 500 °C (user defined)	1 500 °C (user defined)

ence between the density of the metal and oxide layers and the superficial velocity of the gases released in the ablation, which mix the layers and facilitate the homogenization.

The convective heat transfer between the melt and the concrete is calculated on the basis of a distribution of effective heat transfer coefficients along the pool interface in combination with a concrete decomposition temperature. These effective heat transfer coefficients (a proposed set of empirical heat transfer coefficients derived from experiments) are representative for the overall heat transfer from the bulk to the interfaces and are valid for the concrete decomposition temperature specified. The upward heat transfer from the upper interface of the pool to the surrounding is calculated considering radiation and convection processes. A set of proposed HTC was evaluated from ablation rates, observed in a number of 2D MCCI experiments both with homogeneous and stratified melt configuration [9, 10].

The configuration of the melt pool may be fixed without evolution of the core melt or with evolution, i. e. with transition from homogeneous to stratified melt. The criterion for switching from a homogeneous to a stratified configuration depends on the gas flow rate in the melt and is derived from the BALISE experiments [11].

The MELCOR Cavity package is used to model the interactions between core debris and concrete in one or more locations. MCCI calculation modelling is based on CORCON Mod 3 code. It was developed for analysing important core-concrete interaction phenomena, including those that are relevant to the assessment of containment thermal hydraulics and fission product release. Models in CORCON include heat transfer between core debris and concrete, and between core debris and coolant (an overlying water pool). Both homogeneous and stratified melts can be treated by the code. During core-concrete interaction, melt stratification from an initially homogeneous layer is modelled in the code as layer inversion in a stratified geometry. Both gas-phase and condensed-phase chemical reactions are modelled in the code, largely in terms of equilibrium chemistry. The non-equilibrium chemistry model is implemented in the code, but can only be utilized effectively for a very limited number of chemical species. Generation of aerosols and release of fission products are modelled in the code through its VANESA module.

Information about the validation of COCOSYS/CCI (same model basis as MEDICIS) and MELCOR/CORCON is available in [13]. The main models and assumptions in MELCOR/CORCON and COCOSYS/CCI are summarized in Table 1.

4.2 COCOSYS and MELCOR MCCI results

4.2.1 Results for the 60 m^2 spreading area with homogeneous melt

The results for the 60 m^2 spreading area and homogeneous state of the melt are presented in Fig. 8 – Fig. 11. The first two figures depict the ablation of the concrete in radial and axial direction. It is seen that COCOSYS and MELCOR predict practically identical penetration in both directions – around 2.2 m for 60 h. Nevertheless, 60 h after the MCCI initiation, the mass of the melt mixture and ablated concrete in the COCOSYS calculation is around 30 % less than in the MELCOR calculation. This is so because the shapes of the cavities predicted by the codes are different (Fig. 11). The shape of the cavity is determined by the proportion of the ablation in radial and axial direction and by the variation of this proportion in time.

At the very beginning of the ex-vessel phase of the accident the heat exchange between the very hot corium and the cold concrete and air is rather intensive. The temperature of the melt decreases rapidly (Fig. 10). After about one hour the processes become less intensive. The temperature of the melt decreases very slowly and the melt mass increases in constant rate. As was said above, COCOSYS requires user-defined effective heat transfer coefficients in axial and radial direction which are constant in time. The MELCOR model of the heat exchange is more mechanistic. The heat transfer coefficient is calculated by the code in each node of the interface surface and takes into account the change in the properties of the melt and the rate of the gas release from the chemical reactions in the course of the accident. A principal difference between the MELCOR and COCOSYS approaches is that MELCOR uses different HTC at the melt-concrete surface for the different stages of the accident, while COCOSYS uses constant values. In the MELCOR calculation, the heat transfer coefficient for the heat exchange at the pool-concrete interface is rather high (up to 3000 W/(m^2K)) for the initial transient phase of the MCCI and smaller (1000 W/(m^2K)) for the subsequent quasi-stationary phase. COCOSYS applies constant user-defined heat transfer coefficients for the heat exchange between the melt and the concrete in radial and in axial direction. In this case all three HTC are equal to 500 W/(m^2K). These values were recommended by the developers of the CCI module based on MOCKA experiments performed at KIT [3]. In Fig. 11 it can be seen that the shape of the vertical cross section of the cavity shape, predicted by

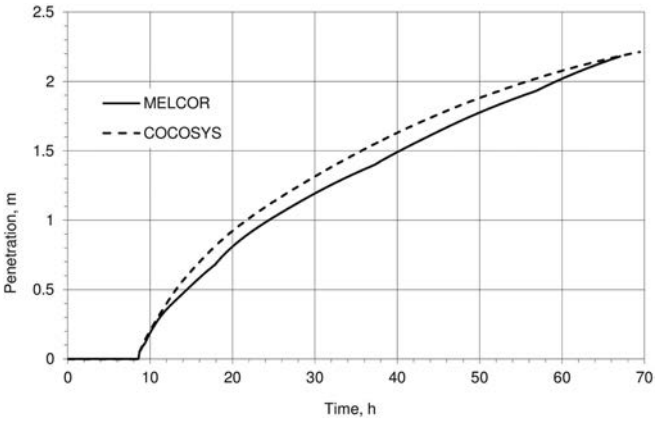

Fig. 8. 60 m2_h Radial penetration

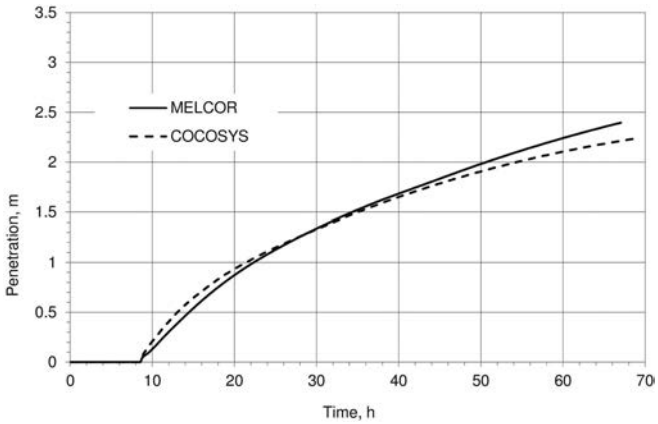

Fig. 9. 60 m2_h Axial penetration

COCOSYS is like a rectangle, which can be explained by the constant and identical in axial and radial direction HTC. The shape of the cross section of the cavity shape, calculated by MELCOR is more like a truncated cone and the depth of the pool is bigger. The higher HTC in the initial phase of the ablation determined in MELCOR calculations are the reason for the conic shape of the cavity.

The heat release from the melt into the concrete is higher in the MELCOR calculation both for the initial transient phase and for the long-term quasi-stationary phase. This corresponds to the higher mass of the melt mixture in MELCOR. In contrast, the heat transferred to the atmosphere is higher in the COCOSYS calculation. As for the heat exchange between the molten pool and the atmosphere, both codes simulate convection and radiation heat exchange. Having in mind the rather high temperatures of the melt, the role of the radiation is more significant. MELCOR assumes a constant effective HTC of 10 W/(m^{2}K) to model the convective heat exchange at top melt surface. COCOSYS calculates the HTC in the range of 15 to 20 W/(m^{2}K). For the radiative heat exchange between the melt and the air and the structures in the cavity MELCOR uses constant emissivity coefficient of 0.6. In the COCOSYS calculation it is 0.9, as recommended in the User guide [1]. At the high temperatures of the melt (Fig. 10), the radiative heat transfer dominates the heat exchange with the atmosphere. The difference in the assumed emissivities is a reason for the different distribution of the power release to the concrete and to the atmosphere in the COCOSYS and MELCOR results. By the end of the calculation, the ratio "power to the concrete"/"power to the atmosphere" is 0.36 for the COCOSYS calculation, while for the MELCOR calculation it is 4.68.

In spite of the different distribution of the released power, both calculations predict almost stationary state i. e. the decay heat and the heat from the chemical reactions are balanced by the heat transferred to the concrete and to the atmosphere. That is why the temperature of the melt mixture decreases very slowly. 60 h after the initiation of the ex-vessel phase of the accident, the temperature of the melt mixture is higher than the ablation temperature. The ablation depth in axial direction is about 2.25 m in CCI (Fig. 9). The thickness of the non-ablated layer of the basement plate is less than 50 cm. Having in mind that the non-ablated layer will be compromised by cracks due to the high temperature gradients, the plate may be considered destroyed under the weight of the ablated mass.

4.2.2 Results for the 60 m^2 spreading area with stratified melt

The results for the 60 m^2 spreading area and stratified state of the melt are presented in Fig. 12 – Fig. 15. For this case the differences between the COCOSYS and MELCOR results are more significant. COCOSYS predicts 1.38 times deeper penetration in radial direction than in axial, while MELCOR predicts that the axial penetration is 1.75 times deeper than the radial penetration (Fig. 12, Fig. 13). The total mass of the melt mixture calculated by COCOSYS is around 40 % less than that calculated by MELCOR. If we look at the shape of the

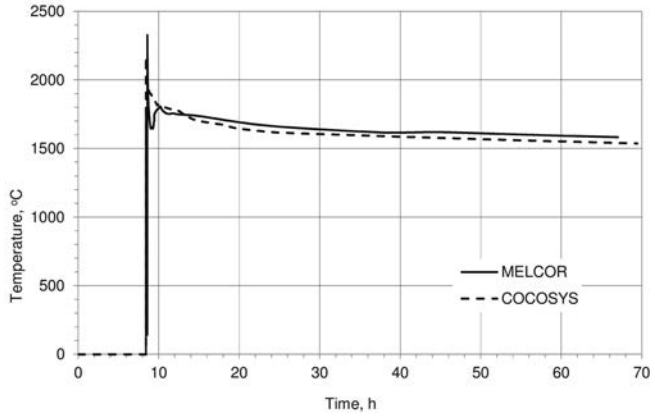

Fig. 10. 60 m2_h Temperature of the melt mixture

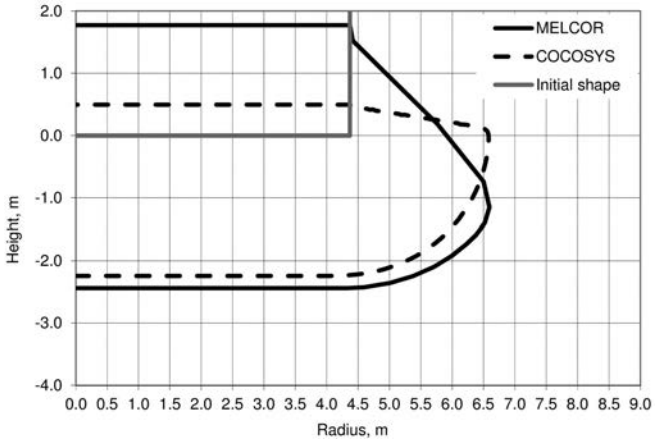

Fig. 11. 60 m2_h Cavity shape

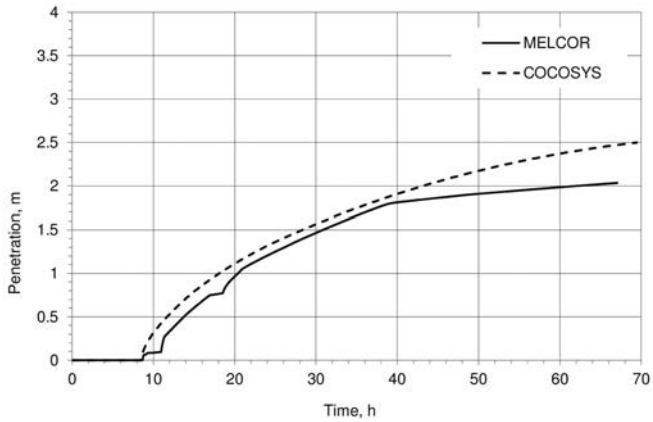

Fig. 12. 60 m2_s Radial penetration

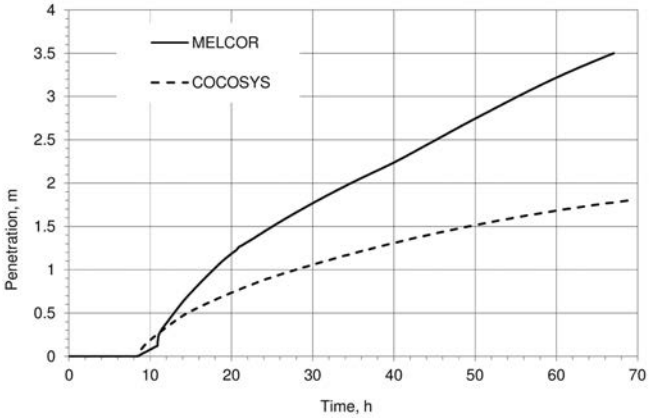

Fig. 13. 60 m2_s Axial penetration

cavity predicted by COCOSYS it is much more extended in radial direction than for the homogeneous case (Fig. 15). The shape of the cavity predicted by MELCOR resembles the one for the homogeneous case, but is jagged, due to the different HTC of the different layers. The faster radial penetration in COCOSYS is due to the fact that the HTC for the metal layer in radial direction is two times higher than in axial direction. This was observed in the recent MOCKA experiments with reinforced concrete [3]. In previous analyses, it was considered that the stratification of a metal layer on the bottom of the mmolten pool causes a more intensive axial ablation because the HTC for the surface metal – concrete is higher than the HTC for the surface oxide-concrete based on previous MOCKA experiments without reinforcement. The MELCOR model also predicts higher HTC and, therefore, higher ablation rates in the axial direction. The definition of a much higher HTC in the radial direction than in axial imposes the fact that a crust is formed on the bottom of the molten pool which reduces the heat transfer to the concrete. This may not always be true. The applicability of experimental results to the reactor cases should be thoroughly discussed. For instance, it should be checked if the ratio between the volume of the melt and the contact surface between the melt and the concrete is as expected for the reactor cases.

Another difference between the COCOSYS and MELCOR is the model for the heat exchange between the metal and oxide layers. In Fig. 14 it is seen that in the MELCOR calculation, the heat transfer between the layers is effective since the temperatures of the metal and oxide phases are the same in the long term. In contrast, in the COCOSYS calculation the heat exchange between the layers is less effective and the temperature of the oxide phase stays higher than the temperature of the metal layer. This is another reason why less heat is transferred to the concrete. It should be kept in mind that the main part of the decay heat is released into the oxide part. For this case the ratio "power to the concrete"/"power to the atmosphere" is 0.35 for the COCOSYS calculation (compared to 0.36 for the homogeneous case). For the MELCOR calculation it is 5.36 (compared to 4.68 for the homogeneous case). In the COCOSYS calculation the stratification of the melt decreases the ablated mass of the melt mixture by 25 tonnes. In contrast, the stratification of the melt intensifies the ablation in the MELCOR calculation. The mass of the ablated concrete increases by 64 tonnes.

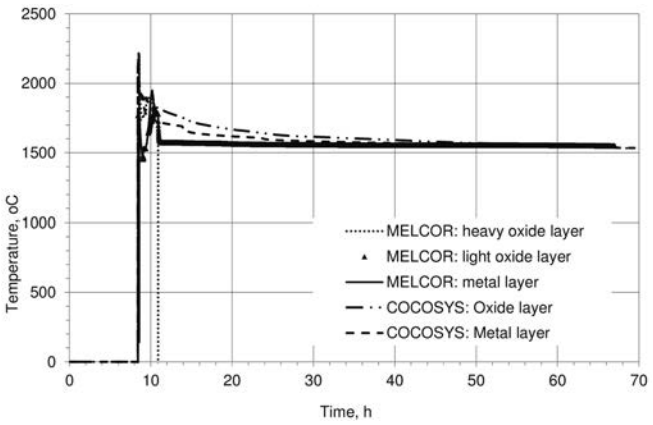

Fig. 14. 60 m2_s Temperature of the melt mixture

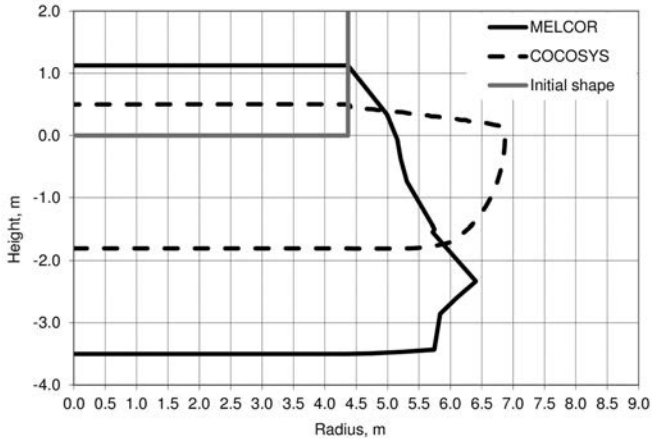

Fig. 15. 60 m2_s Cavity shape

4.2.3 Results for the 100 m^2 spreading area with homogeneous melt

All findings from the comparison between COCOSYS and MELCOR results for the 60 m^2 spreading area and homogeneous state of the melt are also valid here. In spite of the close radial and axial ablation depths calculated by the two codes, the total mass of the melt mixture calculated by COCOSYS is around 35 % less than the mass calculated by MELCOR. Again, COCOSYS predicts that less power is transferred to the concrete than to the atmosphere. The ratio by the end of the calculation is 0.33. In contrast, in the MELCOR calculation this ratio is 4.46, i. e. more power is released into the concrete, than into the atmosphere.

Comparing the 60 m^2 to 100 m^2 COCOSYS results (Fig. 16 – Fig. 19), it can be observed that the larger spreading area leads to a faster decrease of the temperature of the melt and to a less intensive ablation at the beginning of the MCCI. By the end of the calculation, the difference in the temperatures is only 5 °C and the ablation rate is practically the same. The available experimental data confirm quite consistently long-term quasi-stationary temperatures close to 1 600 °C [15].

The difference in the axial and radial penetration between 60 m^2 and 100 m^2 COCOSYS cases is 0.57 m. Though this difference is not negligible, the spreading of the melt over 100 m^2 does not lead to faster cooling of the melt below the ablation temperature. The difference in the mass of the ablated concrete is 9 %.

The comparison between the 60 m^2 and 100 m^2 case for the MELCOR homogeneous calculations also shows that the lar-

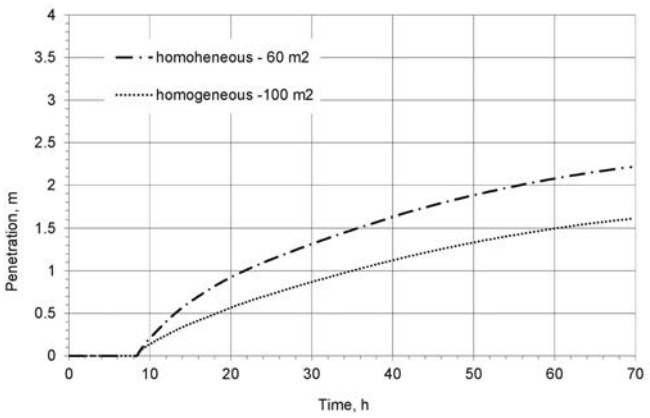

Fig. 16. COCOSYS_60 m2 – 100 m2_h Radial penetration

ger spreading area leads to a faster decrease of the melt temperature in the initial phase, but by the end of the calculation, the difference is about 3 °C. The difference in the total ablated mass is 0.1 %.

4.2.4 Results for the 100 m^2 spreading area with stratified melt

The comparison between COCOSYS and MELCOR for the100 m^2 spreading area and stratified state of the melt leads to similar conclusions as in the case of the 60 m^2 spreading area and stratified melt. COCOSYS predicts 1.4 times deeper penetration in the radial direction than in the axial one, while MELCOR predicts that the axial penetration is 3.7 times deeper than the radial penetration. The mass of the ablated concrete calculated by COCOSYS is around 45 % less than the mass calculated by MELCOR.

Comparing the 60 m^2 to 100 m^2 COCOSYS results (Fig. 20 – Fig. 24), it is seen that the larger spreading area influences the radial penetration more than the axial. The pene-

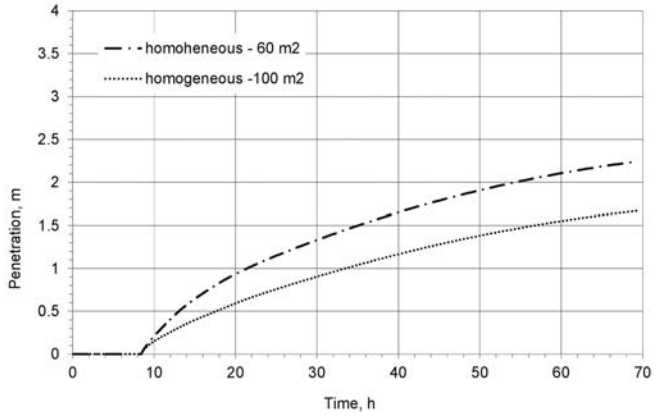

Fig. 17. COCOSYS_60 m2 – 100 m2_h Axial penetration

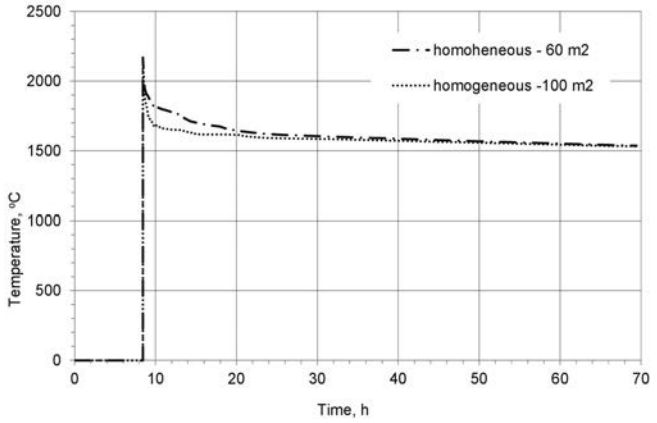

Fig. 18. COCOSYS_60 m2 – 100 m2_h Temperature of the melt mixture

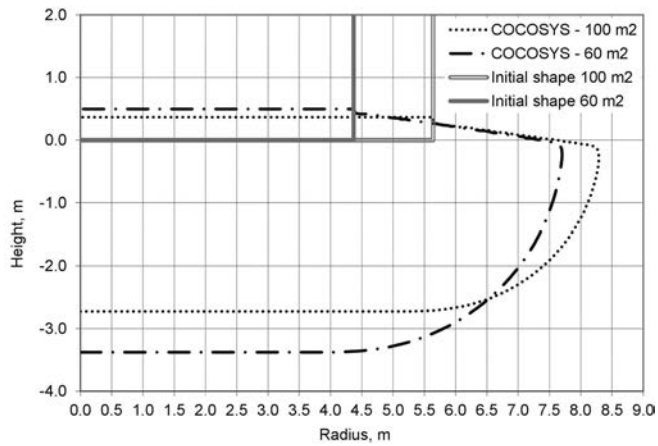

Fig. 19. COCOSYS_60 m2 – 100 m2_h Cavity shape

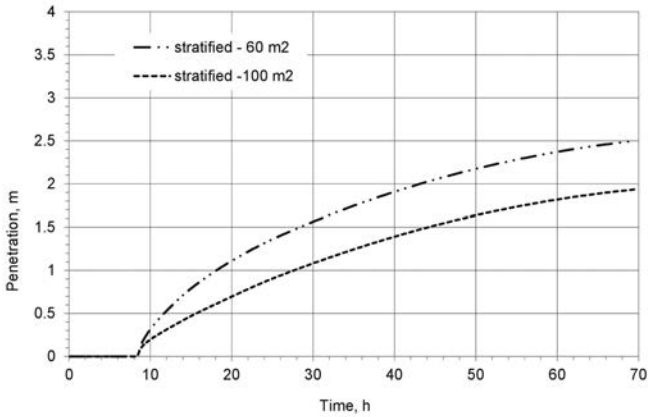

Fig. 20. COCOSYS_60 m2 – 100 m2_s Radial penetration

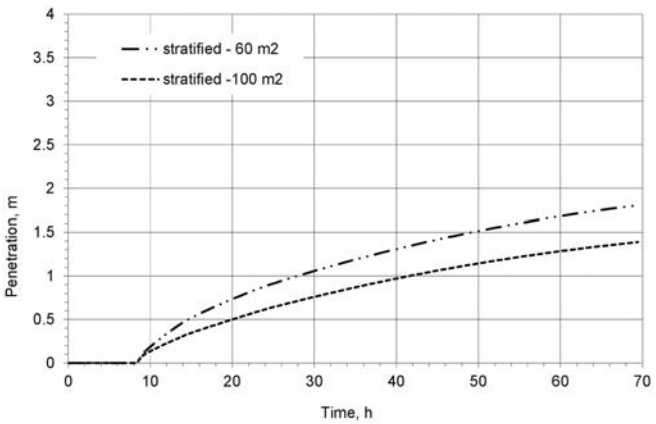

Fig. 21. COCOSYS_60 m2 – 100 m2_s Axial penetration

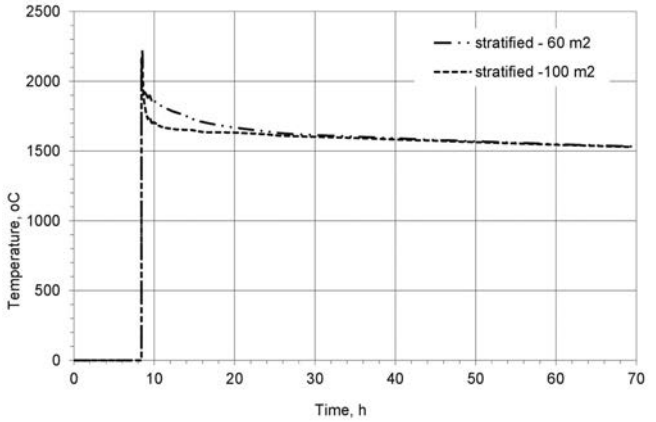

Fig. 22. COCOSYS_60 m2 – 100 m2_s Temperature of the oxide layer

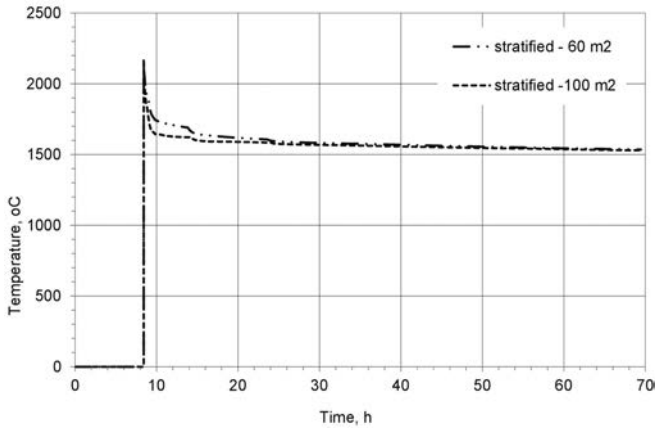

Fig. 23. COCOSYS_60 m2–100 m2_s Temperature of the metal layer

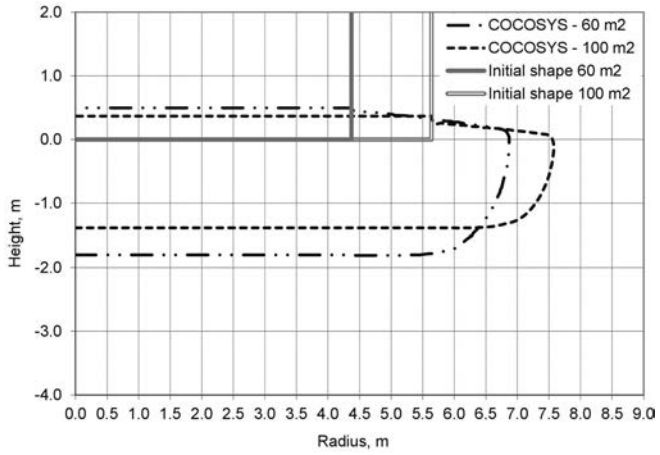

Fig. 24. COCOSYS_60 m2–100 m2_s Cavity shape

tration in the radial direction decreases by 0.57 m, while the penetration in the axial direction decreases by 0.42 m. The difference in the total ablated mass is 8 %. The temperature of the melt is less than 2 °C lower.

The comparison between the 60 m^2 and 100 m^2 cases of the MELCOR stratified calculations also shows that the larger spreading area leads to a faster decrease in the melt temperature in the initial phase, but by the end of the calculation the difference is 16 °C. The difference in the ablated mass is 0.5 %.

The application of the evolutionary model in COCOSYS shows that the stratification takes place 2 h after the initiation of MCCI, which is faster than in the case of the smaller spreading area. The reason is that the ablation in the 100 m^2 case is less intensive in the beginning and fewer gases are released to support the homogenization between the metal and oxide fractions. The long-term results are very similar to the results for the stratified melt.

4.3 Summary of the MCCI results

The MELCOR code predicts more intensive ablation than the COCOSYS code. If the stratification model is applied, MELCOR predicts deeper penetration in the axial direction than COCOSYS, but more shallow penetration in the radial direction than COCOSYS. The COCOSYS MCCI module CCI uses constant effective HTC provided by the user, while the MELCOR MCCI module CORCON calculates them taking into account the properties of the materials, the temperature and the gas release rate. The model used by CORCON for the heat exchange between the metal and oxide layer (Green correlation) predicts a more intensive transfer of the energy from the oxide to the metal layer and further to the concrete than the CCI model. As a result, the COCOSYS calculations predict that more heat is released into the atmosphere than into the concrete. In the MELCOR calculations, more heat is transferred to the concrete than to the atmosphere.

The extrapolation of the 2D MCCI test results to long-term reactor case conditions in terms of convective heat transfer at the corium/concrete interfaces is still an open issue and should be further subject to evaluation and discussion. A valuable source of information is the paper [12].

Both codes predict that the melt temperature decreases rather fast in the initial phase of the MCCI but then the temperature decrease slows down during the quasi-stationary phase.

The increase of the spreading area leads to a faster cooling of the melt in the initial period of the accident, but in the long term the temperatures are the same. The melt is not stabilised. The ablation rate 60 h after the initiation of the ex-vessel phase of the accident is not less than 1 cm/h in both radial and axial direction for all investigated cases (Fig. 16, Fig. 17, Fig. 20 and Fig. 21).

5 Conclusion and outlook

The calculations performed with LAVA with different values of the properties of the molten core materials show that the melt spreads on 60 to 100 m^2. The spreading takes 5 to 10 min, although the melt outflow from the reactor takes longer. The MCCI starts immediately and is very intensive in the beginning. It is advisable to couple LAVA and CCI modules of COCOSYS in order to take into account the correct fraction of the gases in the melt and the change in the viscosity of the melt with the addition of light oxides from the ablated concrete. It is expected that both parameters will influence the spreading.

The duration of the melt release in the experiments [6, 7] is tens of seconds compared to approximately 2 h in the reactor case (80 % of the molten core is released during the first hour). The melt mass is expected to be by a factor of ~330 larger than the experimental one (for ECOKATS-1), which may lead to significantly different ratios between the generated and the accumulated energy on the one hand and the energy transferred to the ambient air and concrete on the other.

It is expected that the difference between T_{liq} and T_{sol} will influence the spreading significantly. So, the influence of this parameter is to be investigated in the future as well.

A similar conclusion regarding future studies is valid for the validation of the CCI module and especially for the applicability of experimental results for determination of the HTC between the molten pool and the concrete. For long term reactor applications it is questionable, if the experimental data base covers sufficiently all relevant scaling issues (area – volume ratio, power to volume scaling etc). It is advisable to improve the simple crust formation model in CCI and to validate it using the existing experiments.

The MELCOR validation status is assumed to be subject of the same uncertainties concerning experiment to real NPP scaling, what is not treated here.

The parallel COCOSYS and MELCOR calculations revealed that the spreading of the melt outside the reactor cav-

ity decreases the intensity of the concrete ablation but it does not lead to a stabilisation of the melt. The results do not allow to recommend opening of the cavity door before a thorough investigation of the direct containment heating consequences is performed.

(Received on 28 January 2019)

References

1 *Klein-Heßling, W.; Arndt, S.; Nowack, H.; Spengler, C.; Schwarz, S.; Eschricht, D.; Beck, S.*: COCOSYS V2.4v5 User's Manual. GRS-P-3/1, Revision 29 July 05, 2018
2 *Spengler, C.*: LAVA 2000, A Computer Code for the Simulation of Melt Spreading in the Containment, Part A: User Manual. (v1.0) GRS-A-2967
3 *Bakalov, I.*: Molten Core-Concrete Interaction, Extended analyses of MCCI processes in WWER-1000/320 applying an increased concrete ablation temperature in COCOSYS CCI module. GRS, INT KoNuS Project meeting, GRS – ENPRO, Work Package 3 December 11–12, 2017
4 *Meyer, L.; Ivanov, I.; Kisyoski, S.; Albrecht, G.; Popov, D.*: Direct Containment Heating (DCH) in VVER 1000 Reactors, Physical Modelling and Experimental Results. Proceedings of Energy Forum, Varna, 2006
5 *Sehgal, B.R.; Dinh, T. N.; Ravva, S. R.*: Severe accident risk assessment and severe accident management, Kozlodouy-5 WWER-1000/V320 plant. Safety evaluation report, Sehgal Konsult, 2005
6 Nuclear safety in light water reactors. Severe accident Phenomenology, Edited by Bal Raj Sehgal, First edition, 2012
7 Test Report of the Melt Spreading Tests ECOKATS-V1 and ECOKATS-1, Forschungszentrum Karlsruhe GmbH, Karlsruhe, 2004
8 U.S. Nuclear Regulatory Commission: An Assessment of the CORCON-MOD3 Code Part I: Thermal-Hydraulic Calculations. NUREG/IA-0129, Part I, September 1996
9 *Spengler, C.*: Validation of the MCCI-Module COCOSYS-MEDICIS. Technical Note, GRS-V-RS1190-1/2012
10 *Cranga, M.; Spengler, C.; Atkhen, K.; Fargette, A.; Fischer, M.; Foit, J.; Gencheva, R.; Guyez, E.; Haquet, J. F.; Journeau, C.; Michel, B.; Mun, C.; Piluso, P.; Sevon, T.; Spindler, B.*: Towards an European Common Understanding of the Causes of MCCI Ablation Anisotropy by an Oxidic Pool. 6th European Review Meeting on Severe Accident Research (ERMSAR-2013), Avignon, October 2013, DOI:10.1016/j.anucene.2014.07.017
11 *Tourniaire, J. B.; Seiler, J. M.; Bonnet, J. M.*: Study of the Mixing of Immiscible Liquids: Results of the BALISE experiments. Proc. of NURETH-10, Seoul, Korea, 2003
12 *Spengler, C.; Fargette, A.; Foit, J.; Agethen, K.; Cranga, M.*: Transposition of 2D Molten Corium-Concrete Interactions (MCCI) from Experiment to Reactor. 6th European Review meeting on Severe Accident Research (ERMSAR-2013) Avignon (France), Palais des Papes, 2–4 October, 2013, DOI:10.1016/j.anucene.2014.07.009
13 *Basu, S.; Bonnet, J.-M.; Cranga, M.; Vola, D.; Farmer, M. T.; Robledo, F.; Spengler, C.*: State-of-the-Art Report on Molten-Corium-Concrete interaction and Ex-Vessel Molten-Core Coolability. OECD/NEA/CSNI Report NEA/CSNI/R(2016)15 (2016)
14 *Spengler, C.; Bakalov, I.; Reinke, N.; Sonnenkalb, M.*: Uncertainty and Sensitivity Analyses in Support of Model Development and Validation of the Containment Module COCOSYS of the AC^2 Code – Application for Molten Corium/Concrete Interaction (MCCI). 12th International Topical Meeting on Nuclear Reactor Thermal-Hydraulics, Operation and Safety (NUTHOS-12), Qingdao, China, October 14–18, 2018
15 *Foit, J. J.; Cron, T.; Fluhrer, B.*: Melt/Concrete Interface Temperature Relevant to MCCI process. The 9TH European Review Meeting on Severe Accident Research (ERMSAR2019), Prague, Czech Republic, March 18–20, 2019

List of abbreviations

AC	Alternating current
DCH	Direct containment heating
HTC	Heat transfer coefficient
MCCI	Molten core-concrete interaction
MCP	Main circulation pump
NPP	Nuclear power plant
RPV	Reactor pressure vessel
SAMG	Severe accident management guidelines
SBO	Station blackout
WWER	Water-cooled water-moderated energy reactor

The authors of this contribution

Nadejda Rijova (corresponding author),
Vanya Saraeva, *Konstantin Gantchev*
E-mail: snr@enproco.com
ENPRO Consult, 107 Cherni Vrah blvd. Sofia, 1407 Bulgaria

Ivan Bakalov, *Holger Wolff*, *Siegfried Arndt*
Gesellschaft für Anlagen- und Reaktorsicherheit (GRS) gGmbH
200 Kurfürstendamm, 10719 Berlin, Germany

Bibliography
DOI 10.3139/124.190010
KERNTECHNIK
84 (2019) 5; page 441–452

ISSN 0932-3902